Formation of Intracellular Concentration Landscapes by Multisite Protein Modification

Javier Muñoz-García,[†*] Boris N. Kholodenko,[†] and Zoltán Neufeld[‡]
[†]Systems Biology Ireland, and [‡]School of Mathematical Sciences and Complex and Adaptive Systems Laboratory, University College Dublin, Belfield, Dublin, Ireland

ABSTRACT Multiple cellular proteins are covalently modified (e.g., phosphorylated/dephosphorylated) at several sites, which leads to diverse signaling activities. Here, we consider a signaling cascade that is activated at the plasma membrane and composed of two-site protein modification cycles, and we focus on the radial profile of the concentration landscapes created by different protein forms in the cytoplasm. We show that under proper conditions, the concentrations of modified proteins generate a series of peaks that propagate into the cell interior. Proteins modified at both sites form activity gradients with long plateaus that abruptly decay at successive locations along the path from the membrane to the nucleus. We demonstrate under what conditions signals generated at the membrane stall in the vicinity of that membrane or propagate into the cell. We derive analytical approximations for the main characteristics of the protein concentration profiles and demonstrate what we believe to be a novel steady-state pattern formation mechanism capable of generating precise spatial guidance for diverse cellular processes.

INTRODUCTION

Cells respond to a range of external cues that are detected by specialized receptors bound to the cell membrane. These signals are processed inside the cell by a web of interlinked signaling pathways to generate specific changes in transcriptional activity of genes in the nucleus. Frequent motifs of signal transduction networks are protein modification cycles (1) in which two opposing enzymes modify a protein, e.g., by phosphorylation and dephosphorylation reactions, respectively. This type of activation of a signaling protein often proceeds through multiple steps by successive modifications at two or more specific residues. Differentially phosphorylated forms have distinct signaling activities. For instance, in the mitogen-activated protein kinase (MAPK) cascade, the Raf-1 kinase phosphorylated on Ser-338 (and other residues in the kinase activation loop) and dephosphorylated on Ser-259 activates the downstream kinase MEK (2,3). However, Raf-1 phosphorylated on Ser-259 (2) is unable to activate MEK, but binds and inhibits the proapoptotic kinase MST2 (4). Similar to the configuration of the MAPK pathway, protein modification cycles typically form a cascade in which the activated form of the protein catalyzes the activation of another protein at the next level of the cascade, and such a scenario repeats at consecutive cascade levels, as shown in Fig. 1.

The stationary signal-response relationships and the temporal dynamics of such cascades have been extensively studied (5–7). It has been shown that multiple cascade levels enhance the response sensitivity to external signals (8) and can produce bistable switches and more complex dynamics in the presence of additional feedback loops in the biochemical interaction network (9,10). Recent theoretical and experimental work has shown that the distribution of proteins can be nonuniform and protein activity gradients can be generated inside the cell (11–15). This is mainly a consequence of the spatial separation of opposing activation/deactivation enzymes, in particular the membrane-localized activation of the protein at the first cascade level and its deactivation in the cytoplasm. The cell response to external cues involves their processing and propagation to distant targets such as the nucleus to modulate transcriptional regulation, and therefore, it is important to understand the spatial distribution of different protein forms and activities, which cannot be captured by the total concentrations. It has been shown previously that localized activation of the signaling cascade at the cell membrane can generate stationary activation profiles (9,16), so that the activation of proteins at each consecutive level propagates more deeply into the cell's interior. This allows for the control of signaling (e.g., with the possibility of cross talk based on spatial computation) and could also play a role in providing cell position or size information to some cellular processes.

The aim of this article is to explore the case of multisite protein modification for spatially distributed signaling cascades and to demonstrate the formation of intricate intracellular landscapes of diverse protein activities relevant to many real signaling pathways. We show that two-site protein modification cycles produce a stationary spatial pattern in which the concentration profiles of the proteins can be very different, depending on their phosphorylation state. Although doubly phosphorylated forms typically generate stationary-front-like structures, monophosphorylated proteins have nonmonotonous concentration profiles with maxima at successive distances from the cell membrane. We derive analytical results for key features of the concentration profiles and determine conditions for robust signal propagation. We also illustrate how the concentration landscape changes with different rate constants for the different levels.

Submitted October 27, 2009, and accepted for publication April 1, 2010.

*Correspondence: javiermunozgarcia@gmail.com

Editor: Herbert Levine.

0006-3495/10/07/0059/8 $2.00

doi: 10.1016/j.bpj.2010.04.014

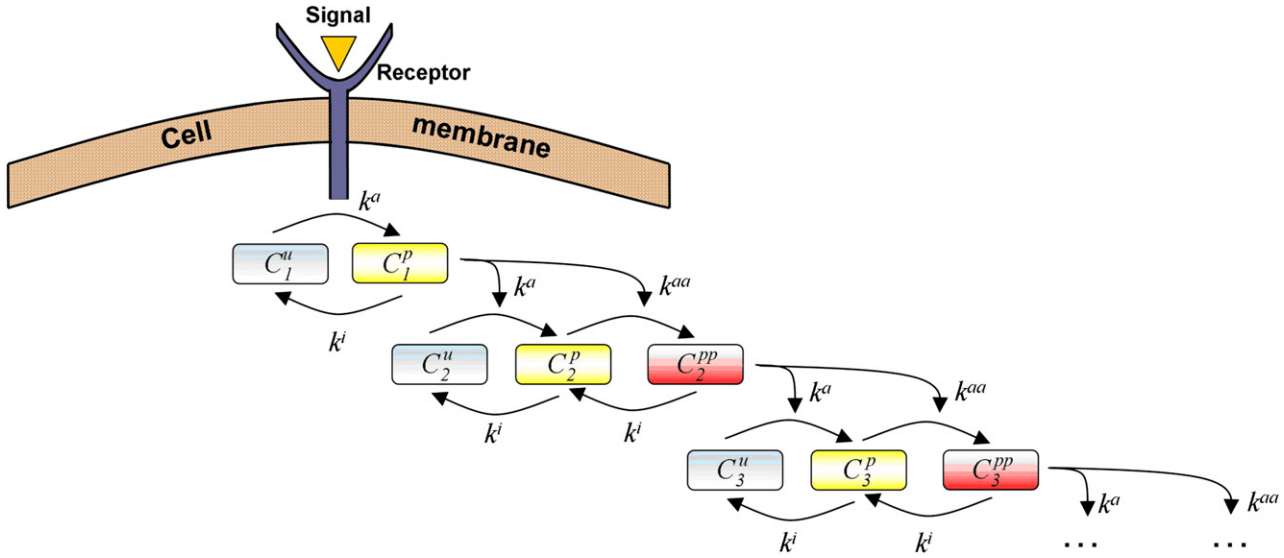

FIGURE 1 Kinetic diagram of a signaling cascade. A protein kinase (C_1) at the first layer is phosphorylated at the cell membrane and dephosphorylated by a phosphatase in the cytoplasm. The doubly phosphorylated form of the kinase (C_n^{pp}) at each subsequent layer (n) phosphorylates the unphosphorylated (C_{n+1}^u) and phosphorylated (C_{n+1}^p) forms of the downstream kinase.

MODEL

We consider a pathway composed of protein modification cycles where proteins are activated and deactivated in two consecutive steps at each cascade level (Fig. 1). The reactions may represent various protein modifications, such as phosphorylation, acetylation, methylation, ubiquitination, etc. For convenience, we use here the terminology of phosphorylation and dephosphorylation reactions. The activation reaction of the first level is catalyzed by a membrane-associated protein (e.g., receptor or bound kinase), whereas at other cascade levels the activation is catalyzed by the active form of the protein from the previous level. The corresponding deactivation reactions are catalyzed by enzymes that are assumed to be uniformly distributed in space.

In a simplified model, which neglects protein sequestration effects, the proteins corresponding to the cascade levels exist in three different forms. Therefore, we can describe the signaling system in terms of the concentrations of the unphosphorylated ($C_n{}^u$), monophosphorylated ($C_n{}^p$), and doubly phosphorylated ($C_n{}^{pp}$) proteins at each level, n, of the cascade. We assume that all the reactions are far from saturation and that the rates are proportional to the substrate and enzyme concentrations. Thus, the concentrations for all levels except the first are given by the equations

$$\frac{\partial C_n^p}{\partial t} = D\Delta C_n^p + k^a C_n^u C_{n-1}^{pp} - k^{aa} C_n^p C_{n-1}^{pp} + k^i C_n^{pp} - k^i C_n^p, \quad n = 2,3,\ldots,N \tag{1}$$

and

$$\frac{\partial C_n^{pp}}{\partial t} = D\Delta C_n^{pp} + k^{aa} C_n^p C_{n-1}^{pp} - k^i C_n^{pp}, \quad n = 2,3,\ldots,N, \tag{2}$$

where D is the diffusion constant and k^a, k^{aa}, and k^i are the effective rate constants corresponding to the activation and deactivation (i.e., phosphorylation and dephosphorylation) reactions. For simplicity, we assume the same dephosphorylation rates for the mono- and doubly phosphorylatyed forms. The first level is different, because it has a single phosphorylation reaction that is only active at the membrane. Thus, the evolution equation for the concentration $C_1{}^p$ lacks the phosphorylation rates and reads

$$\frac{\partial C_1^p}{\partial t} = D\Delta C_1^p - k^i C_1^p. \tag{3}$$

Note that there is an abuse of notation in Eqs. 1 and 2, since for $n = 2$, C_1^{pp} represents the monophosphorylated form that is C_1^p in Eq. 3.

We simplify the analysis by assuming an isotropic spherical cell so that the protein concentrations become functions of the radial distance and time only. We also neglect curvature effects and further consider a one-dimensional reaction-diffusion system with the Cartesian spatial coordinate x. The first protein is activated at the plasma membrane, which corresponds to $x = 0$. For this protein, the diffusive flux at the membrane is determined by the rate of the membrane reaction and is proportional to the concentration of unphosphorylated protein (with proportionality constant υ). The diffusive flux is assumed to be zero at the opposite pole, $x = L$. For kinases at subsequent levels, there is no diffusive flux at either pole, which gives, as boundary conditions for Eqs. 1–3,

$$D\frac{\partial C_1^p}{\partial x}\bigg|_{x=0} = -\upsilon C_1^u\big|_{x=0}, \quad D\frac{\partial C_1^p}{\partial x}\bigg|_{x=L} = 0, \tag{4}$$

and

$$D\frac{\partial C_n^p}{\partial x}\bigg|_{x=0} = D\frac{\partial C_n^{pp}}{\partial x}\bigg|_{x=0} = D\frac{\partial C_n^p}{\partial x}\bigg|_{x=L} = D\frac{\partial C_n^{pp}}{\partial x}\bigg|_{x=L} = 0, \quad n = 2,3,\ldots,N. \tag{5}$$

We have also explored other boundary conditions for the active protein forms at the nuclear membrane that take into account transport through the nuclear membrane, but these produce qualitatively similar behavior and do not affect the propagation of the signal inside the domain.

When the diffusivities, D, of the phosphorylated and unphosphorylated forms are equal and protein synthesis and degradation are negligible on the timescale considered, the total protein abundance at each cascade level is constant across the cell, and we have

$$C_n^u(x,t) + C_n^p(x,t) + C_n^{pp}(x,t) = C_n^{tot}. \tag{6}$$

Thus, we can scale $C_n{}^p$ and $C_n{}^{pp}$ relative to the total concentration at each level and refer to the normalized concentrations of the active components $c_n{}^p = C_n{}^p/C_n{}^{tot}$ and $c_n{}^{pp} = C_n{}^{pp}/C_n{}^{tot}$, bearing in mind that the relative unphosphorylated concentration is given by $1 - c_n{}^p - c_n{}^{pp}$. For the sake of simplicity, we consider the same total concentration for all the levels, C^{tot}. We can nondimensionalize the system, rescaling time and space as $x' \to (D/k^i)^{-1/2}x$ and $t' \to k^i t$. Thus, omitting primes, we obtain from Eqs. 1–3:

$$\frac{\partial c_1^p}{\partial t} = \Delta c_1^p - c_1^p, \tag{7}$$

$$\frac{\partial c_n^p}{\partial t} = \Delta c_n^p + \frac{1}{\gamma^p}\left(1 - c_n^p - c_n^{pp}\right)c_{n-1}^{pp} - \frac{1}{\gamma^{pp}}c_n^p c_{n-1}^{pp} + c_n^{pp} - c_n^p, \quad n = 2,3,\ldots,N, \tag{8}$$

and

$$\frac{\partial c_n^{pp}}{\partial t} = \Delta c_n^{pp} + \frac{1}{\gamma^{pp}}c_n^p c_{n-1}^{pp} - c_n^{pp}, \quad n = 2,3,\ldots,N, \tag{9}$$

where the notation for the dimensionless activation ratio parameters is $\gamma^p = k^i/(C^{tot}k^a)$ and $\gamma^{pp} = k^i/(C^{tot}k^{aa})$, and again there is an abuse of notation when $n = 2$, since by c_1^{pp} we mean c_1^p.

RESULTS

We first study the system behavior numerically, considering activation of the signaling cascade through the cell membrane by an external signal, and we then use the observed qualitative behavior to formulate a more quantitative description. The numerical simulations were done using the pdepe solver in MATLAB for one-dimensional initial-boundary value problems for parabolic-elliptic partial differential equations. We consider that the stimulus is constant on the membrane, so the system can reach its stationary state. The initial conditions correspond to the inactive state $c_n^p(x,t=0) = c_n^{pp}(x,t=0) = 0$. Using typical values for diffusivities and deactivation constants (e.g., $D = 5\ \mu m^2\ s^{-1}$ and $k^i = 4.3\ s^{-1}$, as in Kholodenko (9)), we can estimate the characteristic lengthscale in Eqs. 7–9 as $(D/k^i)^{1/2} \approx 1\ \mu m$. In the numerical simulations, we consider, for illustrative purposes, $N = 5$ cascade levels in a domain that is large enough so that the boundary on the right ($x = L$) does not affect the solutions. Considering five cascade levels allows us to capture the qualitative behavior of a system with an arbitrary number of levels and, since the subsequent levels do not affect the dynamical evolution of the previous levels (see Eqs. 8 and 9), any problem with a smaller number of cascade levels produces the same results for the existing levels. In particular, our results can be considered for the MAPK cascades with only four stages. In a similar way, when the signal propagates and some of the concentration profiles reach the right boundary, the shape of the other signal profiles corresponding to previous cascade levels remain unchanged (see Fig. S1 in the Supporting Material).

For the first level of the cascade, the exact solution is obtained analytically (9,12,16). Specifically, for large domains, the stationary profile is $c_1^p = c_1(0)e^{-x}$, where $c_1(0) = \upsilon/[(Dk^i)^{1/2} + \upsilon]$. This solution depends on the strength of the signal activation at the plasma membrane, υ. In our simulations, we used $\upsilon = (Dk^i)^{1/2}$, so that $c_1(0) = 0.5$. Except for a small region of the parameter space close to the propagation threshold (see below), for most of the parameter values the qualitative behavior of the signal propagation through the cascade and the shape of the concentration profiles at subsequent levels are not very sensitive to the value of $c_1(0)$.

The temporal evolution of the concentration profiles for five consecutive cascade levels is shown in Fig. 2 for the case where $\gamma^p = \gamma^{pp} = 0.01$. Although all concentration profiles of the phosphorylated states propagate into the domain until a stationary distribution is attained, their shapes are qualitatively different for the mono- and doubly phosphorylated forms. In the vicinity of the membrane, proteins at each level are predominantly doubly phosphorylated, whereas phosphorylated forms reach their peaks in the region where there is a sharp decrease of the corresponding doubly phosphorylated forms. For the parameter values considered here, the fifth cascade level reaches up to ~20 μm, which is of the same order of magnitude as the size of a eukaryotic cell.

The stationary concentration profiles for different values of γ^p and γ^{pp} are shown in Fig. 3. When both nondimensional activation parameters are much smaller than unity (i.e., the effective inactivation rates are weaker than the activation rates), the signal always propagates in space through the cascade levels, although the amplitude and relative position of the concentration profiles depend on the parameter values. When both inactivation/activation ratios, γ^p and γ^{pp}, are above unity there is no signal propagation and the concentrations of the phosphorylated forms decay sharply near the left boundary even for a very high stimulus strength.

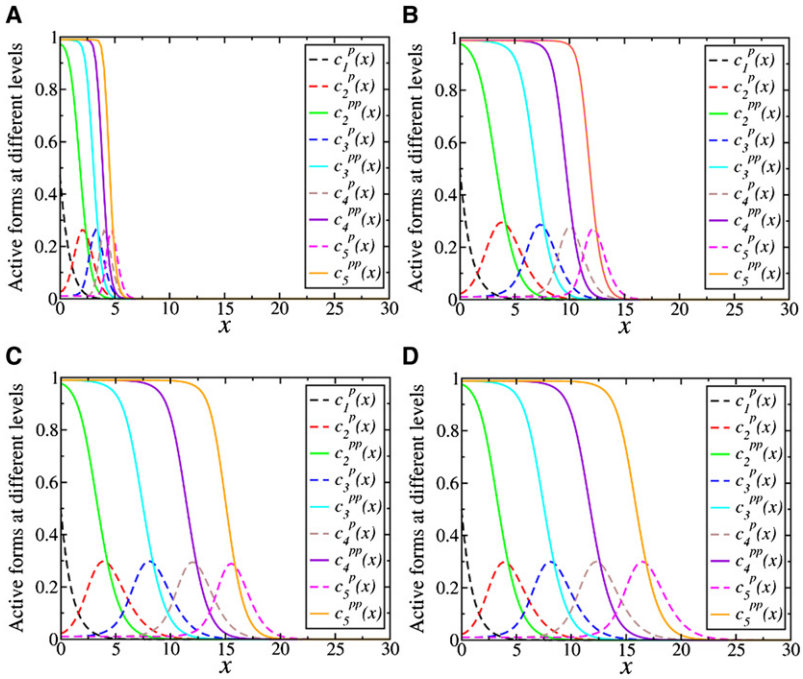

FIGURE 2 Monophosphorylated (*dashed lines*) and doubly phosphorylated (*solid lines*) concentration profiles obtained by numerical integration of Eqs. 7–9 with $\gamma^p = \gamma^{pp} = 0.01$ for the first through fifth (*left to right*) cascade levels at times $t = 1$ (*A*), $t = 5$ (*B*), $t = 10$ (*C*), and $t = 1000$ (*D*).

When the signal propagates, the stationary concentration profile of a doubly phosphorylated protein generates a flat plateau that starts at the plasma membrane (the left boundary) and subsequently decays monotonously to zero in a relatively narrow region whose distance from the plasma membrane increases with the cascade level. The stationary profile of a monophosphorylated form is nonmonotonous; it has a unimodal form, typically with a marked peak. If γ^p is comparable to or larger than γ^{pp} (Fig. 3, *A* and *B*), the concentration peak of the monophosphorylated protein is close to the location of the abrupt decay of the doubly phosphorylated form. When γ^p is slightly larger than unity and $\gamma^{pp} << 1$, the signal still propagates, but the amplitude of the doubly phosphorylated concentration is quite small compared to the maximum of the monophosphorylated protein (Fig. 3 *B*). In general, the relative amplitude of the concentration profiles depends on the ratio γ^{pp}/γ^p, so that larger values give rise to larger amplitude for the monophosphorylated forms. For larger values of γ^{pp}, the doubly phosphorylated concentrations are only activated close to

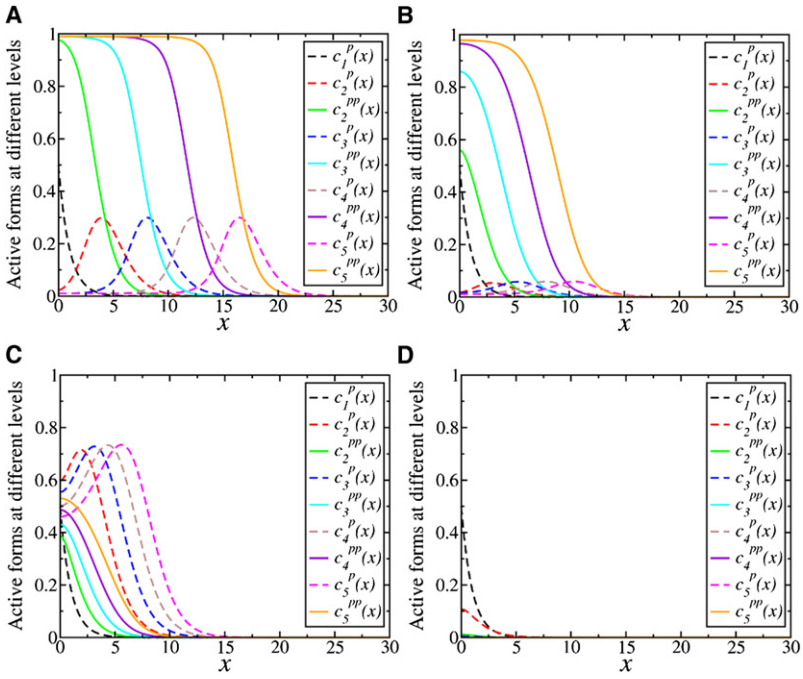

FIGURE 3 Monophosphorylated (*dashed lines*) and doubly phosphorylated (*solid lines*) stationary concentration profiles ($t = 10{,}000$) obtained by numerical integration of Eqs. 7–9 for $\gamma^p = \gamma^{pp} = 0.01$ (*A*), $\gamma^p = 1$, $\gamma^{pp} = 0.01$ (*B*), $\gamma^p = 0.01$, $\gamma^{pp} = 0.4$ (*C*), and $\gamma^p = \gamma^{pp} = 2$ (*D*).

the left boundary, whereas the amplitude and localization of the gradients for the monophosphorylated forms depend on the value of γ^p. For values of γ^p much smaller than γ^{pp}, the monophosphorylated concentrations also form a flat plateau starting from the left boundary for large n, and their amplitude may be even larger than the one corresponding to the doubly phosphorylated concentrations (see Fig. 3 *C*).

A good approximation for the condition for signal propagation can be obtained by assuming that the propagating signal produces a set of similar stationary profiles with flat plateaus on the left side of the domain and that the concentrations at the left boundary, $c^p(x{=}0)$ and $c^{pp}(x{=}0)$, converge to constant values, $c^p(0)$ and $c^{pp}(0)$, for large n (see Fig. 3, *A* and *B*). The existence of concentrations $c^p(x{=}0)$ and $c^{pp}(x{=}0)$ with values in the unit interval [0,1] is therefore a prerequisite for signal propagation. Thus, to obtain concentrations corresponding to the plateau regions, we reduce Eqs. 8 and 9 to

$$\frac{1}{\gamma^p}[1-c^{pp}(0)-c^{pp}(0)]c^{pp}(0)-\frac{1}{\gamma^{pp}}c^p(0)c^{pp}(0) + c^{pp}(0)-c^p(0) = 0, \tag{10}$$

and

$$\frac{1}{\gamma^{pp}}c^p(0)c^{pp}(0)-c^{pp}(0) = 0. \tag{11}$$

From Eq. 11, we have

$$c^p(0) = \gamma^{pp}, \tag{12}$$

and substitution into Eq. 10 gives a quadratic equation for $c^{pp}(0)$:

$$[c^{pp}(0)]^2+(\gamma^{pp}-1)c^{pp}(0)+\gamma^p\gamma^{pp} = 0. \tag{13}$$

Equation 13 has real solutions if the discriminant is positive, $(\gamma^{pp}-1)^2-4\gamma^p\gamma^{pp}\geq 0$, from where we obtain the condition for signal propagation as

$$\gamma^p \leq \frac{(\gamma^{pp}-1)^2}{4\gamma^{pp}}. \tag{14}$$

This curve is represented in Fig. 4 *A* (*dashed line*), where the parameter regions corresponding to propagating (*red crosses*) and decaying (*blue circles*) signals are shown to agree well with the theoretical boundary. (The criterion applied for the classification of stalled or propagating signals in Fig. 4 *A* was based on the sign of $\int_0^L x\times(c_5^{pp}-c_4^{pp})dx$ for the resulting stationary solutions.) As we can see here, the signal propagates for sufficiently small values of γ^p and γ^{pp} (large values of k^a and k^{aa}). In this parameter region, it is found that the doubly phosphorylated stationary solution at the left boundary is well approximated by the larger solution to Eq. 13:

$$c^{pp}(0) = \frac{1-\gamma^{pp}}{2}\left[1+\sqrt{1-\frac{4\gamma^p\gamma^{pp}}{(1-\gamma^{pp})^2}}\right]. \tag{15}$$

Since in this region $\gamma^{pp}<(1-\gamma^p)/2$, it is easy to show that $c^{pp}(0)>c^p(0)$, as expected. We also checked numerically that the concentrations of the mono- and doubly phosphorylated proteins at the left boundary agree well with the analytical predictions given by Eqs. 12 and 15 in this parameter region. In Fig. 4 *B*, we plot the concentrations at $x=0$ measured for the fifth level as a function of γ^{pp} and find that the concentrations agree well with the analytical estimates in the propagating region.

We can gain more insight into the problem, and obtain an analytical approximation for the maximum of the concentration profile of the monophosphorylated protein, by considering a simplified version of the problem in which we neglect the diffusive terms in Eqs. 8 and 9. In this case, the local concentrations of level n can be expressed iteratively as a function of the concentration of the doubly phosphorylated form of the previous level as

$$c_n^p = \frac{\gamma^{pp}c_{n-1}^{pp}}{(c_{n-1}^{pp})^2+\gamma^{pp}c_{n-1}^{pp}+\gamma^p\gamma^{pp}}, \tag{16}$$

and

$$c_n^{pp} = \frac{(c_{n-1}^{pp})^2}{(c_{n-1}^{pp})^2+\gamma^{pp}c_{n-1}^{pp}+\gamma^p\gamma^{pp}}. \tag{17}$$

Using the analytical solution for the first level, $c_1^{pp}(x)=c_1(0)e^{-x}$, these relationships provide a mapping of the concentration profiles from one cascade level to the

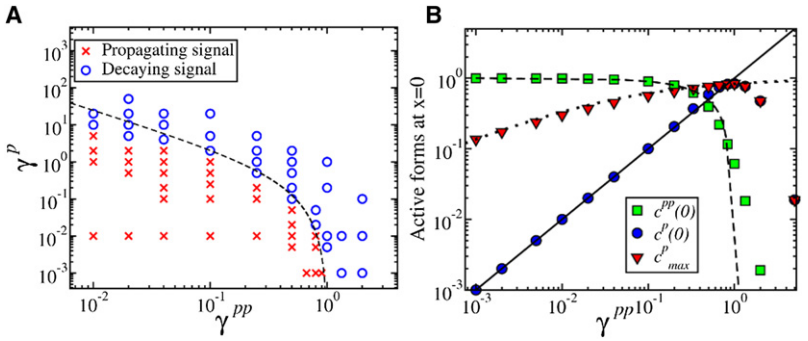

FIGURE 4 (*A*) Parameter regions corresponding to propagating (*red crosses*) and decaying (*blue circles*) signals as a function of γ^p and γ^{pp}, where the dashed line is given by Eq. 14. (*B*) Monophosphorylated (*blue circles*) and doubly phosphorylated (*green squares*) stationary concentrations at $x=0$, $c^p(0)$, and $c^{pp}(0)$, respectively, as a function of γ^{pp} for $\gamma^p=0.01$; the dashed and solid lines correspond to the analytical predictions given by Eqs. 12 and 15, respectively. The red triangles and dotted line represent the maximum of the monophosphorylated form concentration and the analytical prediction given by Eq. 18, respectively.

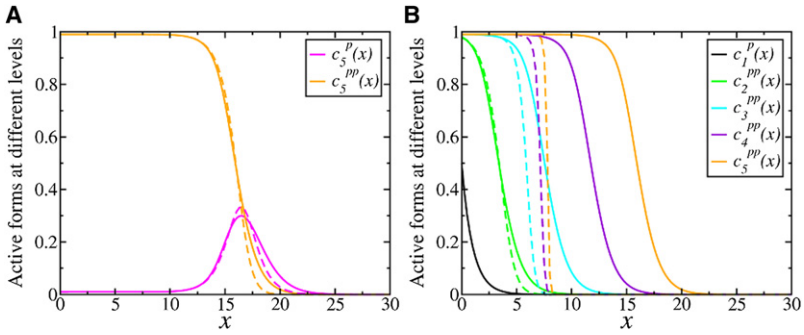

FIGURE 5 (*A*) Stationary monophosphorylated and doubly phosphorylated concentration profiles for the fifth level of the cascade, c_5^p and c_5^{pp}, obtained by numerical simulations, as in Fig. 3 *A* (*solid lines*) and using Eqs. 16 and 17 with c_4^{pp} extracted from Fig. 3 *A* (*dashed lines*). (*B*) Doubly phosphorylated stationary concentration profiles at different levels of the cascade obtained by numerical simulations, as in Fig. 3 *A* (*solid lines*) and using Eq. 17 consecutively with the initial profile, $c_1^p = 0.5e^{-x}$(*dashed lines*).

next. (Note that Eqs. 16 and 17 are also equivalent to the expressions that describe the signal propagation through cascade levels in a spatially uniform system.) In Fig. 5 *A*, we show the concentrations obtained from Eqs. 16 and 17 using the profile of a previous level extracted from our numerical simulations. As observed here, these expressions produce shapes similar to the solutions of the full reaction-diffusion system. However, as we can see in Fig. 5 *B*, where Eq. 17 is applied consecutively using as initial condition the analytical solution for the first level ($c_1^p = 0.5e^{-x}$), when diffusion is neglected, c_n^{pp} tends to a stationary steplike profile for large values of n separating two homogeneous states and does not give a good description for the spatial propagation in the original system. The fact that c_n^{pp} tends to two stable states may be deduced from Eq. 17. This equation describes a bistable mapping with three fixed points corresponding to the three homogeneous stationary solutions of Eqs. 8 and 9 in the limit of $n \to \infty$. The trivial solution $c_n^{pp} = 0$ is stable and the other two solutions are given by a quadratic equation equivalent to Eq. 13. The larger solution is given by Eq. 15 and is a stable state, whereas the other solution is an unstable state limiting the basin of attraction of the other two stable states. As shown above, these solutions are real when the inequality in Eq. 14 is satisfied, which is the parameter range where a propagating solution exists.

The bistable character of the nondiffusive approximation described by Eqs. 16 and 17 gives insight into the dependence of the signal propagation on the strength of the external stimulus at the plasma membrane, represented by the parameter υ in Eq. 4. When the initial profile, $c_1^p(x)$, is everywhere below the unstable fixed point, $c_{unstable}^{pp} = (1-\gamma^{pp})\{1-[1-4\gamma^p\gamma^{pp}/(1-\gamma^{pp})^2]^{1/2}\}/2$, the signal decays even in the parameter region where propagating solutions exist. Thus, in addition to the condition given by Eq. 14, a necessary condition for signal propagation is that, at least, $c_1(0) > c_{unstable}^{pp}$. Although for the spatially nonuniform profiles considered here it is not possible to derive an exact propagation condition as a function of the boundary stimulus parameter, qualitatively one expects that the signal will propagate when the stimulus is sufficiently strong so that the condition $c_1^{pp}(x) = c_1(0)e^{-x} > c_{unstable}^{pp}$ is satisfied over a sufficiently large region of order one near the plasma membrane. Therefore, when Eq. 14 is satisfied, signal propagation will only occur if a sufficiently strong stimulus is applied, whereas in the complementary parameter region, the signal decays near the boundary regardless of the strength of the stimulus. We also note, however, that in the region of robust signal propagation, i.e., when the parameters are sufficiently far from the propagation threshold, the value of the unstable fixed point is very small, and therefore, the signal propagates even for very low values of the boundary reaction rate υ. This explains why we obtained good agreement in Fig. 4 *A* between the theoretical propagation threshold and numerical simulations using a fixed boundary rate corresponding to $c_1(0) = 0.5$.

Another important result obtained from the nondiffusive approximation is based on the observation that the maximum of the concentration profile of the monophosphorylated form can be predicted as the maximum of Eq. 16. Differentiating Eq. 16 with respect to c_{n-1}^{pp} and setting the derivative to zero, we find that the maximum of c^p is reached for $c_{n-1}^{pp} = \sqrt{\gamma^p\gamma^{pp}}$ and has the value of

$$\max_x c_n^p(x) = \frac{1}{1+2\sqrt{\frac{\gamma^p}{\gamma^{pp}}}}, \tag{18}$$

which is independent of the shape of the activation profile of the previous level. When $\gamma^{pp} << \gamma^p$, the second phosphorylation step is much faster than the first, and therefore, the concentration of the monophosphorylated form is low and the maximum is close to zero. In the opposite case, $\gamma^{pp} >> \gamma^p$, the second phosphorylation reaction is much slower, and therefore, the protein accumulates in the intermediate state and the maximum is close to unity. As shown in Fig. 4 *B*, the expression in Eq. 18 gives a good approximation to the numerical results when signal propagates into the cell.

It is also interesting to estimate the normalized total amount of doubly phosphorylated form obtained as the integral of c_n^{pp} over the whole domain, that we denote by $\overline{c_n^{pp}}$, which gives a measure of the distance of propagation from the cell membrane, L_n, since $\overline{c_n^{pp}} \propto c_n^{pp}(0)L_n$. In Fig. 6 *A*, the total amount of doubly phosphorylated protein, $\overline{c_n^{pp}}$, is plotted as a function of the cascade level for different values of $\gamma^{pp} = \gamma^p$. As we can clearly see here, the total amount of active protein is a linear function of the cascade level n.

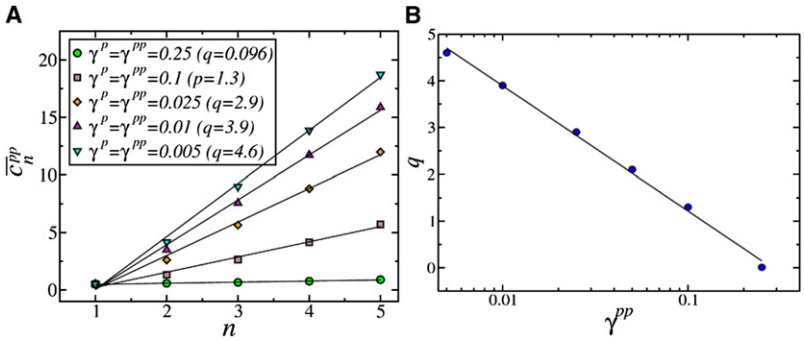

FIGURE 6 (*A*) Stationary normalized total concentration $\overline{c_n^{pp}}$ as a function of n for different values of $\gamma^p = \gamma^{pp}$. The solid lines are the corresponding linear fit to the data and q is the resulting slope. (*B*) The obtained slope, q, as a function of $\gamma^p = \gamma^{pp}$, with the x axis on a logarithmic scale. The solid line is the curve $q = 1.16\log(1/\gamma^{pp}) - 1.45$.

This means that the propagation distance of the front increases approximately linearly with n. From a linear fit, we can obtain the slope q for different values of γ^p and γ^{pp}. In Fig. 6 *B*, we observe that this slope decreases logarithmically with γ^{pp} in a manner similar to the case of a cascade of single phosphorylation cycles, previously studied in Muñoz-García et al. (16).

We have assumed so far that the ratio of the rate constants of deactivation to activation is the same for all levels. This allowed us to gain some intuition and to obtain analytical results, but in general, the activation and deactivation rates can be different for the different cascade levels. Different reaction rates can produce a more complex concentration landscape and spatial patterns. Although a systematic study of all possible concentration patterns is beyond the scope of this article, illustrative examples are shown in Fig. 7. Here, we show the stationary concentration profiles for five cascade levels, where levels 2, 4, and 5 have the same low deactivation/activation ratio that allows signal propagation ($\gamma^p = \gamma^{pp} = 0.01$), but level 3 can impede the spreading of the signal. As can be seen in Fig. 7 *A*, if the values of γ_3^p and γ_3^{pp} are large enough, signal propagation is halted. An interesting property of this system is that even for values of γ_3^p and $\gamma_3^{pp} > 1$, the signal can jump over the third layer and propagate further if γ_3^p and γ_3^{pp} are not too large. This is shown in Fig. 7 *B*, where $\gamma_3^p = \gamma_3^{pp} = 10$. Here, we can see that the third-level kinase is almost completely inactive, but because there is still some active form available, the signal can reach the subsequent cascade levels. A more complex scenario is found for different deactivation/activation rate constant ratios for the mono- and doubly phosphorylated forms. Two such examples are shown in Fig. 7, *C* and *D*, where $\gamma_3^p = 0.1$, $\gamma_3^{pp} = 10$ and $\gamma_3^p = 10$, $\gamma_3^{pp} = 0.1$, respectively. If the ratio of deactivation and activation rates is larger for the second phosphorylation of the target kinase, Fig. 7 *C* shows that the maximum of the phosphorylated form decreases, whereas the profile for the doubly phosphorylated form is similar to the rest of the doubly phosphorylated kinases, although with a smaller amplitude. In contrast, Fig. 7 *D* shows that the maximum of phosphorylated concentration at the third level is almost the same as at the other levels

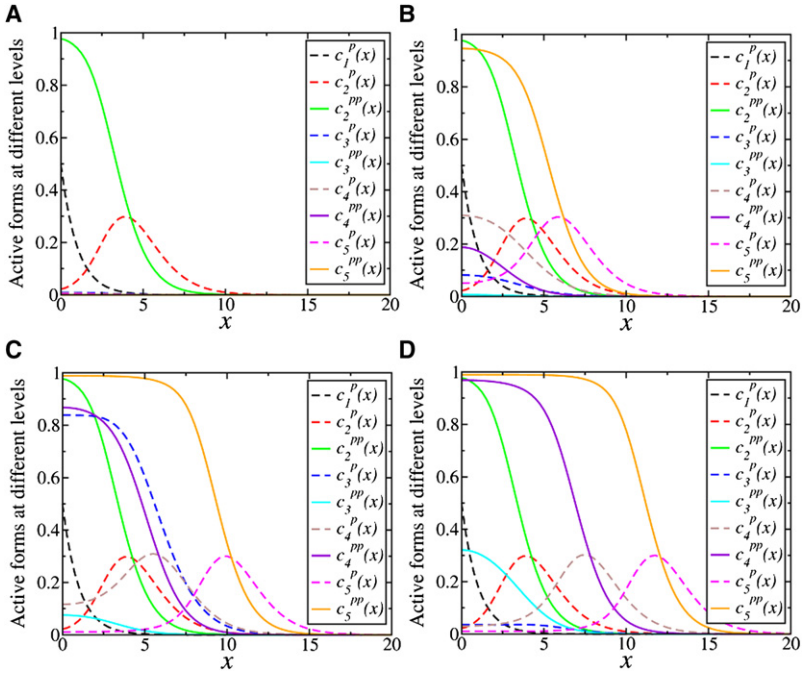

FIGURE 7 Monophosphorylated (*dashed lines*) and doubly phosphorylated (*solid lines*) stationary concentration profiles obtained by numerical integration of Eqs. 7–9 with $\gamma^p = \gamma^{pp} = 0.01$, except at the third level, which is set to $\gamma_3^p = \gamma_3^{pp} = 100$ (*A*), $\gamma_3^p = \gamma_3^{pp} = 10$ (*B*), $\gamma_3^p = 0.1$, $\gamma_3^{pp} = 10$ (*C*), and $\gamma_3^p = 10$, $\gamma_3^{pp} = 0.1$ (*D*).

(although it is shifted to the left), whereas the doubly phosphorylated form at the third cascade level almost vanishes.

DISCUSSION

Multisite protein modifications play a key role in the regulation of cellular functions by signaling pathways (9,17,18). Here, we show that spatially distributed cascades create intricate concentration landscapes of signaling proteins that can control the spatial organization of intracellular processes. Depending on the ratios of the rate constants for phosphorylation and dephosphorylation reactions, the signal may decay in the vicinity of the plasma membrane or propagate inside the cell to distant cellular targets. We have shown previously that for a cascade with monophosphorylated proteins, active protein forms can generate a set of stationary concentration fronts with broad plateaus that decay abruptly at successive spatial locations toward the nucleus (16). Remarkably, this key feature of signal propagation persists for multisite phosphorylation cascades. We demonstrated that at proper activation/deactivation rate constants for the successive cascade levels, the concentrations of doubly phosphorylated signaling proteins propagate into the cell interior without decay and then abruptly descend to basal levels, so that downstream levels of the cascade extend for longer distances.

A novel feature of the multisite modification system is the nonmonotonous behavior of the intermediate protein form, with maximum concentration typically reached in the region where the concentration of the fully activated form decays. We obtained approximate analytical expressions for the conditions of signal propagation and for the main features of the generated concentration landscapes. Numerical simulations show good agreement with approximate analytical solutions. These characteristic spatial distributions can provide positional information to other biochemical pathways in the cell, identifying specific regions with well-defined distances from the plasma membrane.

The results presented here are based on some simplifying assumptions. We neglected the saturation of the reaction rates and assumed linear dependence on the enzyme and substrate concentrations. In the case of Michaelis-Menten-type reaction rates, we expect to obtain qualitatively similar behavior, although in that case the resulting equations for the propagation conditions cannot be solved explicitly. Nevertheless, the propagation conditions obtained here for the linear case remain valid as a limiting case when the saturation constants are sufficiently large.

We have also shown that more complex concentration profiles can form when the reaction rates are not the same at all cascade levels. For example, when the propagation condition is not satisfied at an intermediate level, the further propagation of the signal, both in space and to higher cascade levels, may be suppressed. Such effects could be used in regulating cross talk between different signaling pathways. Evolutionary tuning of the reaction parameters, and additional feedback loops, may allow for complex spatial regulation of the signal propagation.

SUPPORTING MATERIAL

One figure is available at http://www.biophysj.org/biophysj/supplemental/S0006-3495(10)00475-3.

This work was supported by grants from Science Foundation Ireland (06/CE/B1129) and the National Institutes of Health (GM059570). B.N.K. is a Science Foundation Ireland Stokes Professor of Systems Biology.

REFERENCES

1. Seet, B. T., I. Dikic, …, T. Pawson. 2006. Reading protein modifications with interaction domains. *Nat. Rev. Mol. Cell Biol.* 7:473–483.
2. Dhillon, A. S., S. Meikle, …, W. Kolch. 2002. Regulation of Raf-1 activation and signalling by dephosphorylation. *EMBO J.* 21:64–71.
3. von Kriegsheim, A., A. Pitt, …, A. S. Dhillon. 2006. Regulation of the Raf-MEK-ERK pathway by protein phosphatase 5. *Nat. Cell Biol.* 8:1011–1016.
4. Romano, D., D. Matallanas, …, W. Kolch. 2010. Proapoptotic kinase MST2 coordinates signaling crosstalk between RASSF1A, Raf-1, and Akt. *Cancer Res.* 70:1195–1203.
5. Goldbeter, A., and D. E. Koshland, Jr. 1981. An amplified sensitivity arising from covalent modification in biological systems. *Proc. Natl. Acad. Sci. USA.* 78:6840–6844.
6. Heinrich, R., B. G. Neel, and T. A. Rapoport. 2002. Mathematical models of protein kinase signal transduction. *Mol. Cell.* 9:957–970.
7. Kholodenko, B. N., J. B. Hoek, …, G. C. Brown. 1997. Quantification of information transfer via cellular signal transduction pathways. *FEBS Lett.* 414:430–434.
8. Ferrell, Jr., J. E. 1997. How responses get more switch-like as you move down a protein kinase cascade. *Trends Biochem. Sci.* 22:288–289.
9. Kholodenko, B. N. 2006. Cell-signalling dynamics in time and space. *Nat. Rev. Mol. Cell Biol.* 7:165–176.
10. Qiao, L., R. B. Nachbar, …, S. Y. Shvartsman. 2007. Bistability and oscillations in the Huang-Ferrell model of MAPK signaling. *PLOS Comput. Biol.* 3:1819–1826.
11. Berezhkovskii, A. M., M. Coppey, and S. Y. Shvartsman. 2009. Signaling gradients in cascades of two-state reaction-diffusion systems. *Proc. Natl. Acad. Sci. USA.* 106:1087–1092.
12. Brown, G. C., and B. N. Kholodenko. 1999. Spatial gradients of cellular phospho-proteins. *FEBS Lett.* 457:452–454.
13. Kalab, P., K. Weis, and R. Heald. 2002. Visualization of a Ran-GTP gradient in interphase and mitotic *Xenopus* egg extracts. *Science.* 295:2452–2456.
14. Maeder, C. I., M. A. Hink, …, M. Knop. 2007. Spatial regulation of Fus3 MAP kinase activity through a reaction-diffusion mechanism in yeast pheromone signalling. *Nat. Cell Biol.* 9:1319–1326.
15. Stelling, J., and B. N. Kholodenko. 2009. Signaling cascades as cellular devices for spatial computations. *J. Math. Biol.* 58:35–55.
16. Muñoz-García, J., Z. Neufeld, and B. N. Kholodenko. 2009. Positional information generated by spatially distributed signaling cascades. *PLoS Comput. Biol.* 5:e1000330.
17. Markevich, N. I., J. B. Hoek, and B. N. Kholodenko. 2004. Signaling switches and bistability arising from multisite phosphorylation in protein kinase cascades. *J. Cell Biol.* 164:353–359.
18. Thomson, M., and J. Gunawardena. 2009. Unlimited multistability in multisite phosphorylation systems. *Nature.* 460:274–277.